

## **CHAPTER - 8**

---

# **APPLICATION OF STABLE ISOTOPE FOR DECIPHERING GROUNDWATER RECHARGE PATTERNS IN THE KHAPRI WATERSHED**

# APPLICATION OF STABLE ISOTOPE FOR DECIPHERING GROUNDWATER RECHARGE PATTERNS IN THE KHAPRI WATERSHED

## 8.1 Introduction

Stable isotopes of oxygen ( $^{16}\text{O}$  and  $^{18}\text{O}$ ) and hydrogen ( $^1\text{H}$  and  $^2\text{H}$ ) are integral components of a water molecule and are used as tracers for decoding the intricacies of water movement throughout the hydrological cycle (Deshpande et al., 2003a; Deshpande, Maurya, Kumar, et al., 2013a; Deshpande & Gupta, 2012a). The importance of stable water isotope applications in hydrological studies are well known and discussed in literature reported over the past few decades (Bhattacharya et al., 1985, 2003; Chandrasekharan et al., 1992; Dalai et al., 2002; Das et al., 1988; Datta et al., 1991; Datta, Bhattacharya, et al., 1996; Datta, Deb, et al., 1996; Deshpande et al., 2003b, 2010; Deshpande, Maurya, Angasaria, et al., 2013; Deshpande, Maurya, Kumar, et al., 2013b; Deshpande & Gupta, 2012b; Gupta et al., 2005; Gupta & Deshpande, 2003, 2005; B. Kumar et al., 1982, 2010; Maurya et al., 2011; Navada et al., 1993; Navada & Rao, 1991; Nijampurkar et al., 2002; Pande et al., 2000; Purushothaman et al., 2014; Rai et al., 2009; Ramesh & Sarin, 1992; Saha et al., 2013; Sarin et al., 1992; Sengupta & Sarkar, 2006; Shivanna et al., 2004, 2008; Singh et al., 2010; Srivastava et al., 2007, 2010, 2012; Sukhija et al., 1998; Unnikrishnan Warriar et al., 2010; Yadav, 1997).

The application of oxygen and hydrogen isotopes should be treated as a valuable and essential tool in hydrological investigations rather than just sophistication. The stable isotope studies hold excellent potential to fill the knowledge gaps in operations of hydrological systems. The outcome of such studies enables efficient management of stressed water resources and meet the increasing water demand for various civil requirements (Gupta & Deshpande, 2004; R. Kumar et al., 2005). Moreover, the improved understanding about water related natural processes and their monitoring using isotope approach can prove useful to strengthen the sustainable water resource development and management strategy. The stable isotopes are highly useful in revealing the origin of the water, residence time in the subsurface, mixing processes, groundwater contamination and recharge patterns (Praveen, 2015). An important application of isotopes ( $\delta^{18}\text{O}$  and  $\delta^2\text{H}$ ) is to unveil possible relationships existing between the aquifers and surface water bodies (Gray et al., 2019). Thus, the subtle hydrogeological processes

which otherwise are difficult to understand with common hydrometric approach can be easily understood through stable isotope techniques.

For the sustainable development of groundwater resources in the Khapri watershed an attempt has been made to decipher the groundwater recharge from various sources such as rainfall, surface water and spring water, using the stable isotope approach.

### 8.2 Water sampling for stable isotope analysis

For isotope analysis the groundwater samples are collected during May-2022 (37 Nos.) and January-2023 (37 Nos.) from the wells which are in daily use. In addition to groundwater samples, the rainwater (5 Nos. in August 2022) and river water samples (12 Nos. in September-2022 and January-2023) are also collected and analysed for stable isotopes of Oxygen and Hydrogen. The samples for stable isotope analysis are stored in the HDPE bottles of 100 ml capacity with inner stubs. The HDPE bottles are filled upto the top with no space inside and are closed tightly to avoid evaporative loss and associated isotope fractionation. To collect the rainwater samples, 5 rainwater collection units were setup at villages viz, Ghodi, Dhulchond, Malin, Galkund and Gadhvi (Figure 8.1). The collected water samples are analysed for stable isotope of oxygen and hydrogen at Physical Research Laboratory (PRL), Ahmedabad.

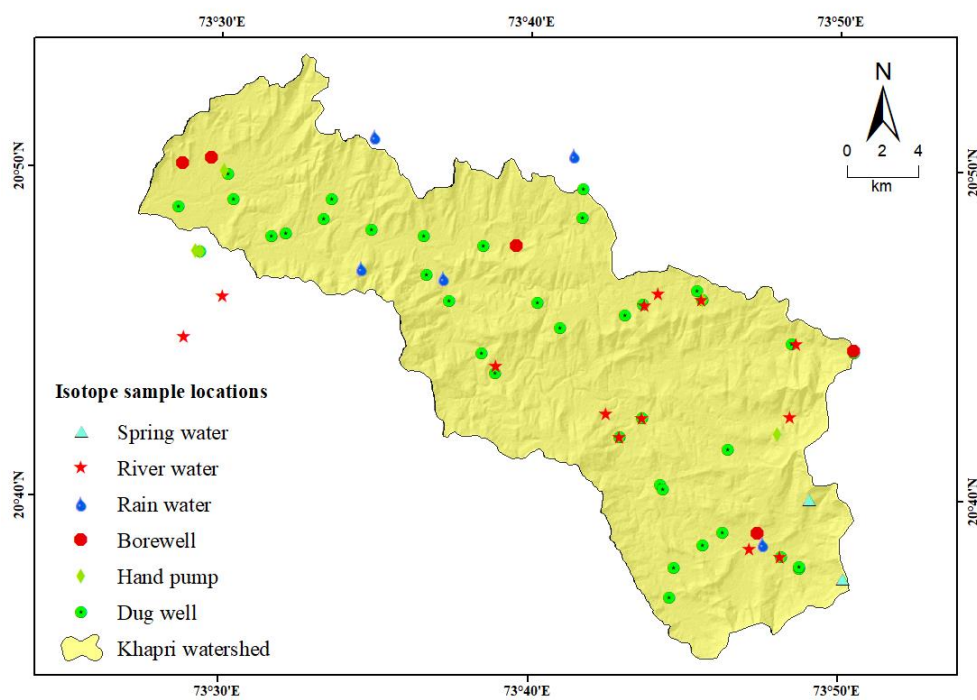


Figure 8.1 Water sampling locations for stable isotope analysis.

### 8.3 Stable isotopes analysis

The stable isotope composition of various water samples is analysed through isotope ratio mass spectrometer (IRMS). The analysis is based on the fundamental principle of mass spectrometry, where the gaseous molecules are ionized and are separated into a spectrum, based on the mass to charge ratio under the influence of electric and magnetic fields. In IRMS the temperature, electric and magnetic fields are kept constant and at the same time the relative intensity of ion beams is measured. The IRMS can measure the mass to charge ratio ranging from 2 to 100 and is instrumented to generate intense steady beams in low-noise Faraday cups for high precision (Praveen, 2015). Initially, the samples are equilibrated with gases such as CO<sub>2</sub>, N<sub>2</sub>, SO<sub>2</sub> and H<sub>2</sub>. The isotopologues of such gases get together in the Faraday cups depending upon the variations in their deflections because of constant electric and magnetic fields (Praveen, 2015).

For analysing the <sup>18</sup>O/<sup>16</sup>O and D/H ratios to compute δ<sup>18</sup>O and δ<sup>2</sup>H values, the water samples are equilibrated with CO<sub>2</sub> and H<sub>2</sub> gases respectively through gas equilibration method (Epstein and Mayeda, 1953). Such equilibrated gas with isotopic expression of water is then introduced into isotope ratio mass spectrometer (IRMS) Delta V plus (figure 8.2) in continuous flow mode with the help of Gas bench II at Physical Research Laboratory (PRL), Ahmedabad. In continuous flow mode the sample preparation and the consequent analysis is performed online in continuous flow of helium. Gas bench is digitally controlled automatic arrangement which converts the water samples into a gas to be introduced to the mass spectrometer. The measurements of <sup>18</sup>O/<sup>16</sup>O and D/H ratios are carried out against the standards recommended by the international atomic energy agency (IAEA), Vienna (Gonfiantini, 1978). The repeated analysis of the multiple aliquots of standards has provided the reproducibility of 0.1 ‰ for δ<sup>18</sup>O and 1 ‰ for δ<sup>2</sup>H.

The isotopic composition is expressed in terms of the abundance ratios of the heavy to light oxygen and hydrogen stable isotopes ( $R = {}^{18}\text{O}/{}^{16}\text{O}$  and D/H) (Oza et al., 2020). The δ<sup>18</sup>O and δ<sup>2</sup>H ( $= (R_{\text{sample}}/R_{\text{std}} - 1) \times 1000$ , where R<sub>std</sub> is the ratio of Vienna Standard Mean Ocean Water [VSMOW]) is reported in parts per thousand or per mil (‰) notation. In addition to these two delta values, the additional parameter i.e. d-excess

( $= \delta^2\text{H} - 8 \times \delta^{18}\text{O}$ ) is determined, which indicates the kinetic fractionation related with the different water samples.



**Figure 8.2 Isotope Ratio Mass Spectrometer (IRMS) at Physical Research Laboratory (PRL), Ahmedabad.**

#### **8.4 Stable isotope composition of rainwater and the meteoric water line for the Khapri watershed**

Local meteoric water line (LMWL) is a graphical representation of the relationship existing between the isotopic composition of precipitation and surface or groundwater for a specific region. To generate the local meteoric water line (LMWL), five rainwater samples collected from Khapri watershed are analysed for  $\delta^2\text{H}$  ‰ and  $\delta^{18}\text{O}$  ‰. The  $\delta^{18}\text{O}$  values of rainfall sample vary from -8.0 to -2.6 ‰ with an average of -4.3 ‰ (table 8.1). The linear regression equation obtained for the LMWL of above rain samples is  $\delta^2\text{H} = 7.86 \delta^{18}\text{O} + 9.97$  with correlation coefficient of  $R^2 = 0.99$  (figure 8.3). The slope of the LMWL is very close to the slope of global meteoric water line (GMWL) ( $\delta^2\text{H} = 8 \delta^{18}\text{O} + 10$ ) (Craig, 1961) as well as the slope of LMWL of Ahmedabad ( $\delta^2\text{H} = 7.8 \delta^{18}\text{O} + 8$ ) (Oza et al., 2020). However, the Y-intercept of LMWL of Khapri watershed is less than GMWL, but greater than the LMWL of Ahmedabad. This indicates the rainfall in and around Khapri watershed is enriched in heavy isotopes as compared to Ahmedabad.

**Table 8.1 Results of  $\delta^{18}\text{O}$ ,  $\delta^2\text{H}$  and d-excess of different water samples.**

Pre-monsoon groundwater samples							
Sample no.	Location	Lat.	Long.	Sampling date	$\delta^{18}\text{O}$ ‰	$\delta^2\text{H}$ ‰	d-excess
3	Chichigavtha	20.81	73.55	5/22/2022	-1.96	-9.69	6.0
4	Dhadhra	20.82	73.56	5/22/2022	-1.78	-6.42	7.8
5	Malin	20.80	73.58	5/22/2022	-1.36	-4.19	6.7
6	Chikatiya	20.80	73.61	5/22/2022	-1.98	-7.32	8.5
7	Bhavandagad	20.77	73.62	5/22/2022	-1.98	-9.42	6.4
8	Golasta	20.74	73.64	5/22/2022	-1.28	-2.95	7.3
9	Sunda	20.73	73.65	5/22/2022	6.84	30.25	-24.5
16	Dhulchond	20.74	73.62	5/22/2022	-2.39	-8.69	0.9
18	Mulchond	20.76	73.58	5/22/2022	-1.63	-5.18	11.0
20	Ghogli	20.76	73.58	5/22/2022	-1.91	-7.46	9.1
21	Gaykhas	20.76	73.60	5/21/2022	-2.32	-10.60	4.7
22	Bhisya	20.78	73.61	5/21/2022	0.61	1.56	10.5
23	Mahalpada	20.80	73.66	5/21/2022	-1.27	-9.08	3.0
24	Pipalghodi	20.79	73.64	5/21/2022	-2.01	-6.20	7.9
25	Ahwa	20.77	73.65	5/22/2022	-2.28	-10.84	0.2
26	Temburgartha	20.77	73.67	5/21/2022	3.07	13.43	7.8
27	Temburgartha	20.76	73.72	5/21/2022	2.33	9.49	7.9
29	Vihiramba	20.77	73.73	5/20/2022	-1.55	-7.77	-3.3
30	Vihiramba	20.77	73.76	5/20/2022	-1.49	-5.68	1.0
33	Lahancharya	20.77	73.76	5/20/2022	-1.48	-5.79	9.9
35	Dhumkhal	20.75	73.68	5/20/2022	-2.33	-12.59	7.4
36	Jakhana	20.71	73.73	5/20/2022	-1.72	-9.06	-11.1
37	Jakhana	20.70	73.72	5/20/2022	-1.45	-6.97	-9.14
38	Pipalpada	20.67	73.74	5/20/2022	1.22	2.53	4.7
40	Mohpada	20.67	73.74	5/20/2022	-1.48	-1.82	6.2
41	Mohpada	20.65	73.77	5/20/2022	-1.01	-6.19	6.1
44	Linga	20.64	73.78	5/20/2022	-1.17	-5.41	5.3
47	Kudkas	20.64	73.76	5/20/2022	-1.63	-5.83	6.1
48	Kudkas	20.63	73.75	5/21/2022	-1.97	-15.78	4.7
50	Chikar	20.62	73.74	5/21/2022	-0.62	-1.68	4.6
54	Borigavtha	20.64	73.80	5/22/2022	-1.86	-11.38	-7.2
55	Vati	20.63	73.80	5/22/2022	-1.49	-8.09	0.8
56	Vati	20.63	73.81	5/22/2022	-1.70	-5.35	10.1
58	Jamanvahir	20.63	73.81	5/19/2022	-1.07	-5.07	1.9
60	Chankhal	20.69	73.77	5/19/2022	-1.47	-7.08	3.9
61	Pandva	20.71	73.77	5/19/2022	-1.08	-5.43	3.65
62	Morzira	20.80	73.53	5/19/2022	0.19	-0.56	7.18
Rain water samples							
1	Ghodi	20.85	73.58	Aug-22	-3.11	-15.48	9
2	Dhulchond	20.78	73.62	Aug-22	-8.06	-53.46	11
3	Galkund	20.64	73.79	Aug-22	-2.67	-10.71	11
4	Malin	20.78	73.58	Aug-22	-3.57	-17.38	11
5	Gadhvi	20.84	73.69	Aug-22	-3.93	-21.02	10

Surface water samples							
S-9	Sunda	20.73	73.65	1/7/2023	-0.82	-5.12	1
S-22	Bhisya	20.77	73.73	1/5/2023	-1.59	-14.51	-2
S-23	Mahalpada	20.77	73.76	1/5/2023	-1.64	-15.60	-3
S-26	Temburgartha	20.71	73.73	1/5/2023	-1.45	-13.73	-2
S-27	Temburgartha	20.70	73.72	1/5/2023	-0.85	-10.70	-4
S-39	Pipalpada	20.64	73.80	1/6/2023	-2.16	-16.47	1
S-61	Pandva	20.75	73.81	1/5/2023	-1.83	-12.47	2
L-1	Bhisya Dam	20.77	73.74	9/26/2022	-3.07	-21.84	3
L-2	Pandava	20.75	73.48	9/26/2022	-2.88	-19.82	3
L-3	Anjanikund	20.71	73.81	9/26/2022	-3.39	-19.28	8
L-4	Galkund	20.64	73.79	9/26/2022	-2.65	-15.79	5
L-5	Borkhel	20.71	73.71	9/26/2022	-2.21	-17.08	1
L-6	Dodipada	20.77	73.50	9/26/2022	-2.53	-13.70	7
Post-monsoon groundwater samples							
6	Chikatiya	20.80	73.61	1/7/2023	-1.67	-10.54	3
8	Golasta	20.74	73.64	1/7/2023	-2.26	-10.63	9
9	Sunda	20.73	73.65	1/7/2023	-2.26	-10.50	3
21	Gaykhas	20.76	73.60	1/5/2023	-1.63	-5.49	11
23	Mahalpada	20.80	73.66	1/5/2023	-2.06	-7.13	9
24	Pipalghodi	20.79	73.64	1/5/2023	-0.86	-4.06	10
25	Ahwa	20.77	73.65	1/5/2023	-2.20	-9.33	10
26	Temburgartha	20.77	73.67	1/6/2023	-2.67	-12.63	7
27	Temburgartha	20.76	73.72	1/5/2023	-2.14	-10.48	9
29	Vihiramba	20.77	73.73	1/5/2023	-2.71	-10.50	11
30	Vihiramba	20.77	73.76	1/5/2023	-2.44	-10.23	9
33	Lahancharya	20.77	73.76	1/5/2023	-2.85	-10.74	11
35	Dhumkhal	20.75	73.68	1/6/2023	-3.14	-13.29	8
36	Jakhana	20.71	73.73	1/6/2023	-2.47	-14.55	9
37	Jakhana	20.70	73.72	1/6/2023	-1.85	-8.45	8
38	Pipalpada	20.67	73.74	1/6/2023	-2.44	-9.48	5
40	Mohpada	20.67	73.74	1/6/2023	-3.10	-16.53	5
41	Mohpada	20.65	73.77	1/6/2023	-2.45	-11.10	3
44	Linga	20.64	73.78	1/6/2023	-2.62	-11.37	5
47	Kudkas	20.64	73.76	1/6/2023	-2.25	-7.22	7
48	Kudkas	20.63	73.75	1/4/2023	-2.45	-8.71	8
50	Chikar	20.62	73.74	1/7/2023	-2.53	-11.90	3
54	Borigavtha	20.64	73.80	1/7/2023	-2.55	-15.01	-11
55	Vati	20.63	73.80	1/7/2023	-2.62	-18.42	-11
56	Vati	20.63	73.81	1/4/2023	-2.55	-15.86	-11
58	Jamanvahir	20.63	73.81	1/4/2023	-2.43	-10.50	11
60	Chankhal	20.69	73.77	1/7/2023	-2.17	-7.57	12
61	Pandva	20.71	73.77	1/5/2023	-3.08	-13.53	10
62	Morzira	20.80	73.53	1/5/2023	-3.16	-16.52	9

Handpump samples							
51A	Vati	20.79	73.49	5/19/2022	-1.68	-1.86	12
56	Vati	20.79	73.49	1/4/2023	-2.29	-8.08	10
57	Sukmal	20.70	73.80	1/7/2023	-2.38	-8.87	10
66	Dungarda	20.83	73.50	1/7/2023	-2.17	-8.15	9
Bore well samples							
51A	Halmundi	20.84	73.49	5/19/2022	-1.91	-7.94	7
52	Amania	20.84	73.48	5/19/2022	-1.84	-1.95	13
59	Isdar	20.79	73.66	5/21/2022	-1.81	14.39	29
59	Isdar	20.79	73.66	1/7/2023	-2.47	-10.46	9
62	Morzira	20.74	73.84	5/21/2022	-2.12	-9.32	8
64	Morzira	20.74	73.84	1/6/2023	-2.84	-12.74	10

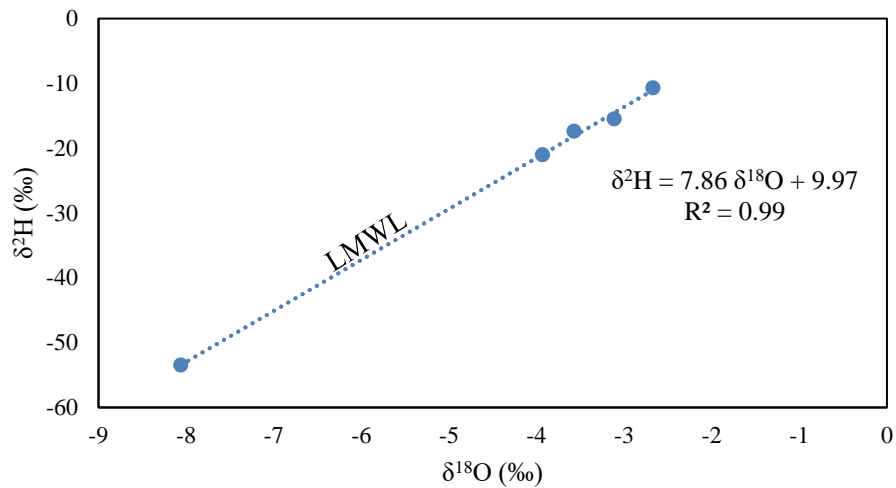
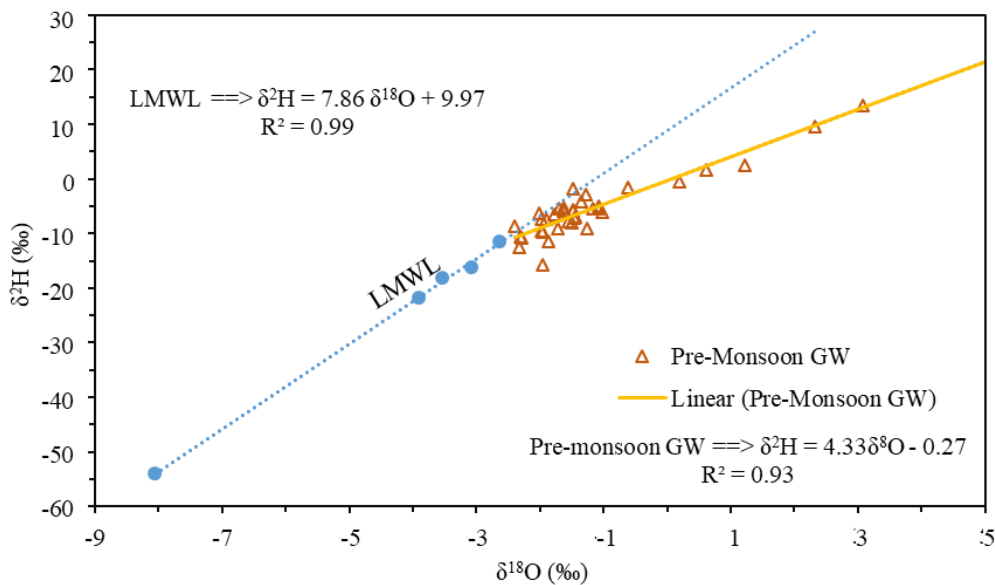


Figure 8.3 LMWL of the Khapri watershed.

### 8.5 Stable isotope composition of groundwater and river water samples

Pre-monsoon groundwater samples collected from open-dug wells showed variation in  $\delta^{18}\text{O}$  from -2.4 ‰ to 1.2 ‰ with an average value of -0.9 ‰, while the groundwater collected from deeper sources such as hand pump and bore-well have  $\delta^{18}\text{O}$  of -1.6 ‰ and -2.1 ‰ to -1.8 ‰ respectively (table 8.1). The linear regression equation obtained for the pre-monsoon groundwater samples is  $\delta^2\text{H} = 4.33 \delta^{18}\text{O} - 0.27$  with correlation coefficient of  $R^2 = 0.93$  (figure 8.4). The slope for the linear regression equation of pre-monsoon groundwater samples is less than the slope obtained for the LMWL. This suggests that the groundwater samples are subjected to evaporation leading to enrichment of  $\delta^{18}\text{O}$  and decrease in values of d-excess (figure 8.5). However, the relatively negative values of  $\delta^{18}\text{O}$  in pre-monsoon dug-well samples could be suspected for the recharge from the return flow of deeper groundwater sources (hand-pumps and

bore wells) which are mined during this period to sustain agriculture. On the other hand, the post-monsoon groundwater samples from open-dug wells showed variation in  $\delta^{18}\text{O}$  from -3.0 ‰ to -0.8 ‰ with an average of -2.4 ‰. The  $\delta^{18}\text{O}$  of post-monsoon groundwater samples collected from hand pump ranges between -2.3 ‰ to -2.1 ‰, while the samples from bore well range from -2.8‰ to -2.4 ‰ (table 8.1). The linear regression equation of post-monsoon groundwater samples is  $\delta^2\text{H} = 5.13 \delta^{18}\text{O} + 1.21$  with correlation coefficient  $R^2 = 0.55$  (figure 8.6). The slope for the linear regression equation of post-monsoon groundwater samples is greater than the slope obtained for the pre-monsoon groundwater samples but less than that of LMWL. This indicates the reduction in the  $\delta^{18}\text{O}$  and increase in d-excess values with respect to pre-monsoon groundwater samples (figure 8.5). This may be on account of the influx of fresh water recharging the groundwater during post-monsoon season. The samples which fall below the regression line of LMWL (figure 8.6) indicate that the groundwater is mixed with rain water which has undergone evaporation prior to recharge. This is supported by the relative enrichment of  $\delta^{18}\text{O}$  and decrease in values of d-excess (figure 8.5). The  $\delta^{18}\text{O}$  values of river water shows variation between -3.3 to -0.8 ‰ with an average of -2.1 ‰ (table 8.1). The river water samples are falling below the LMWL (figure 8.7), indicating the evaporation of the river water after the rainfall in the post-monsoon season.



**Figure 8.4 Scatter plot of  $\delta^2\text{H}$  versus  $\delta^{18}\text{O}$  ‰ for pre-monsoon groundwater samples of the Khapri watershed and LMWL indicates the local meteoric water line.**

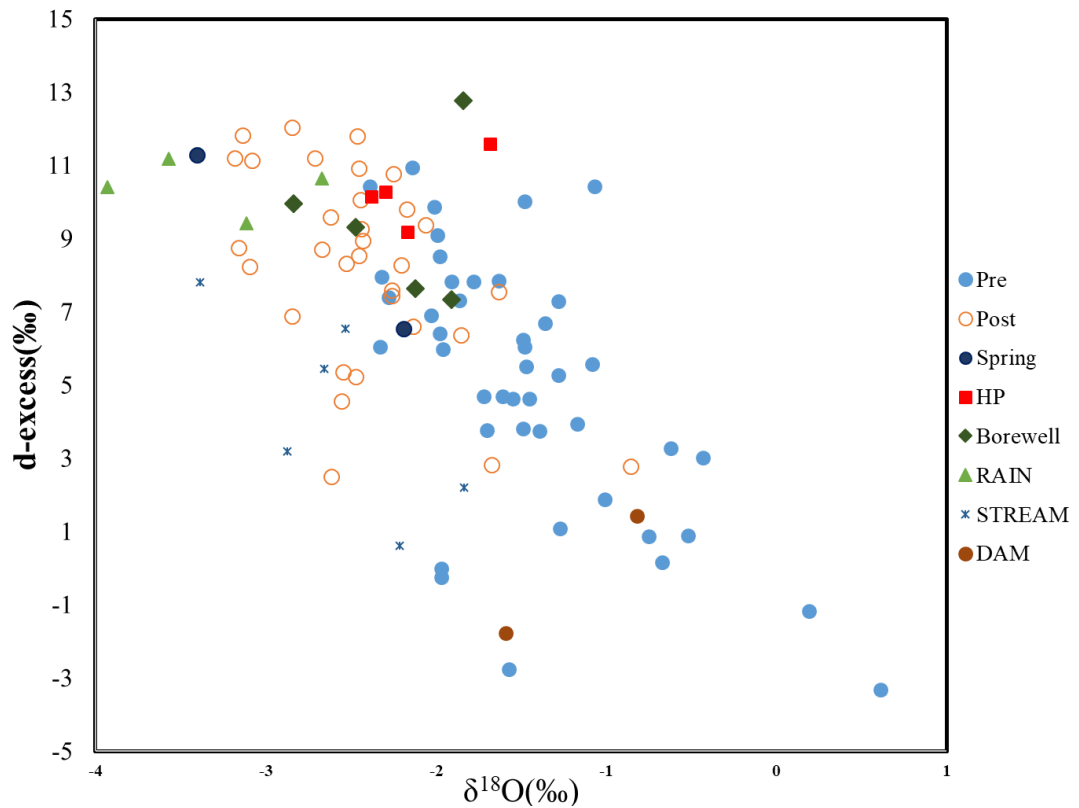


Figure 8.5 Scatter plot of d-excess versus  $\delta^{18}\text{O}$  ‰ for different water samples of the Khapri watershed.

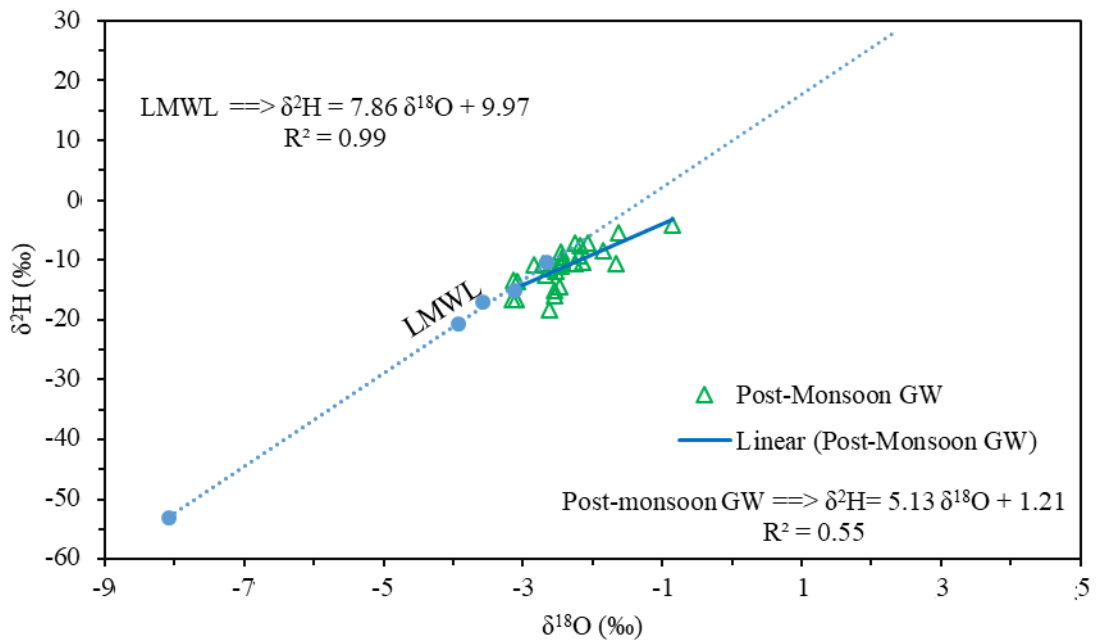
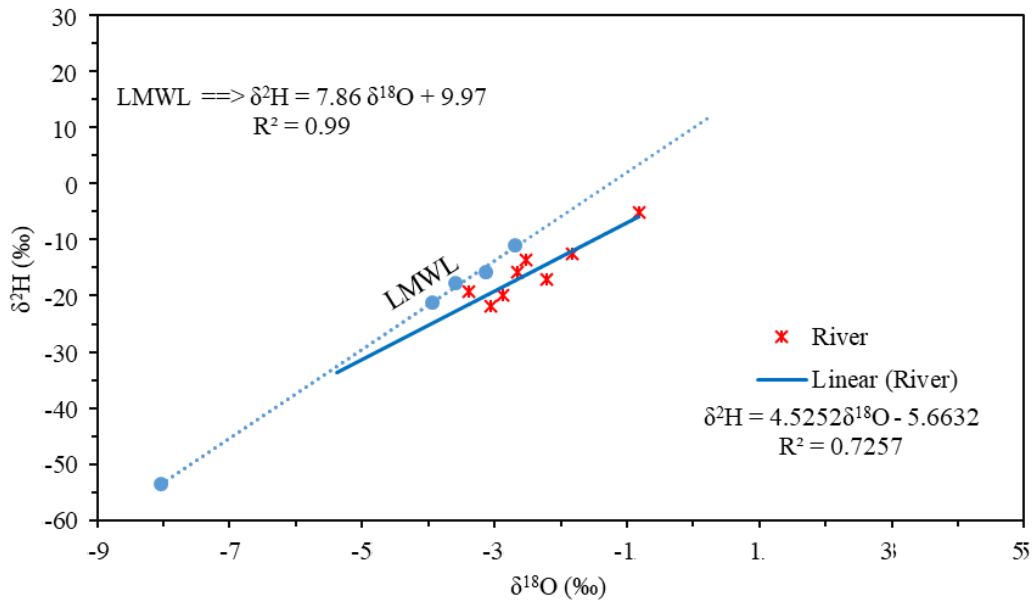


Figure 8.6 Graph of  $\delta^2\text{H}$  versus  $\delta^{18}\text{O}$  ‰ for post-monsoon groundwater samples of the Khapri watershed and LMWL indicates the local meteoric water line.



**Figure 8.7** Scatter plot of  $\delta^2\text{H}$  versus  $\delta^{18}\text{O}$  for river water samples of the Khapri watershed and LMWL indicates the local meteoric water line.

### 8.6 Salient features of stable isotope analysis

To decipher the groundwater recharge patterns the rain water, river water and seasonal groundwater samples are collected from different locations in the Khapri watershed (figure 8.1). The stable isotope composition of different water samples is given in table 8.1.

1) The depletion of -8.0 ‰ in  $\delta^{18}\text{O}$  of rainfall samples indicate the vapour has travelled much inland from its source i.e. the Arabian Sea during southwest monsoon.

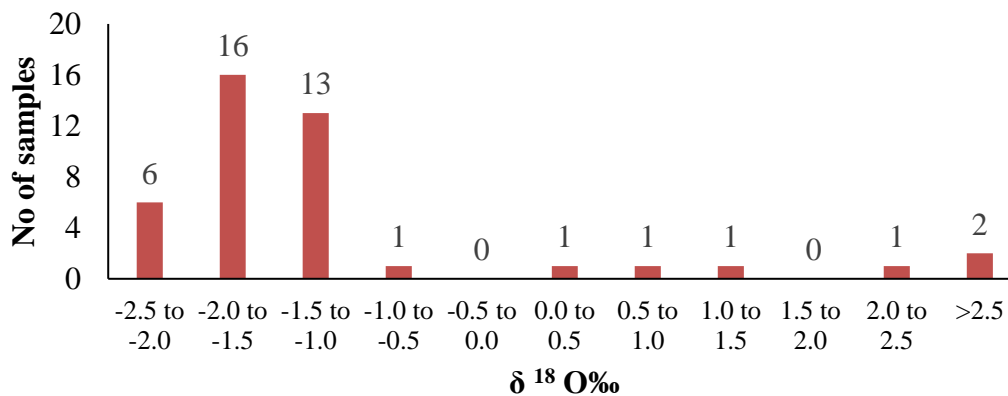


**Figure 8.8** Frequency distribution of  $\delta^{18}\text{O}$ ‰ in pre-monsoon groundwater samples.

2) The frequency distribution histogram of  $\delta^{18}\text{O}\text{‰}$  shows that around 86 % of pre-monsoon groundwater samples of Khapri watershed are in the range of -2.5‰ to -0.5 ‰ (figure 8.8).

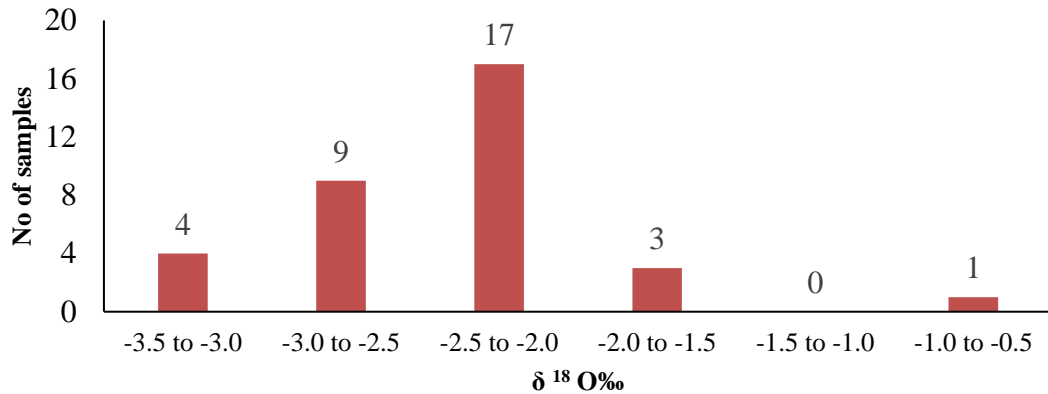


**Figure 8.9** Frequency distribution of  $\delta^{18}\text{O}\text{‰}$  in post-monsoon groundwater samples.

3) For post-monsoon groundwater samples, the frequency distribution histogram of  $\delta^{18}\text{O}\text{‰}$  shows that around 88 % samples are in the range of -3.5‰ to -2.0 ‰ (figure 8.9).

4) The wells located in upper reaches (> 450 m asl) show  $\delta^{18}\text{O}\text{‰}$  enrichment in comparison to wells located in the lower reaches (< 450 m asl). From this it can be inferred that the wells in the upper reaches and steeply sloping terrain, forms the recharge zones for the wells in the lower reaches. Ultimately, the wells in upper reaches are now left with the residual water which is eventually getting evaporated and resulting into the relative enrichment of  $\delta^{18}\text{O}\text{‰}$ .

5) Four pre- and post-monsoon dug well samples are collected from the regions near to surface water bodies such as Themburgartha and Bhisya dam shows enrichment (0.2 ‰ to 2.3 ‰) and depletion (-3.1 to -2.1 ‰) of  $\delta^{18}\text{O}$  respectively. The enrichment of  $\delta^{18}\text{O}$  in pre-monsoon dug well sample is on account of the recharge that has taken place through the water in the dams which has undergone evaporation. The depletion in  $\delta^{18}\text{O}$  of post-monsoon dug well samples may be on account of the new influx of rainwater (-4.3 ‰) to the dams.

6) The pre-monsoon dug well samples show relative enrichment of  $\delta^{18}\text{O}$  with respect to post-monsoon dug well samples indicating evaporation. This is also supported by the decreasing d-excess values from post to pre-monsoon. While, in post-monsoon samples

the depleted values of  $\delta^{18}\text{O}\text{‰}$  and increasing d-excess values suggest influx of fresh water on account of precipitation.

7) The stable isotope data of deeper groundwater collected from hand-pump and bore well shows negative values of  $\delta^{18}\text{O}$  in both pre- (-1.68 ‰) as well as post-monsoon seasons (-2.38 ‰ to -2.17 ‰), which suggests that the recharge of the phreatic aquifers is taking place from the agriculture return flow of deeper groundwater which is being utilized for the farming during non-rainy seasons and similar is also observed for south Gujarat by Pandey et al. (2023).

The stable isotope study highlights four groundwater recharge patterns through different sources viz. (i) Meteoric water which directly infiltrates through negative lineaments that act as a conduit for recharging the shallow groundwater aquifers (ii) Rivers and reservoirs recharge the shallow groundwater aquifers through water percolation (iii) Springs which are recharging the surrounding wells throughout the year and (iv) Deeper groundwater from the bore-wells and hand-pumps used for agriculture, constitutes the return flow for recharging the shallow groundwater aquifers. With this background of groundwater recharge pattern, a further emphasis is given to augment the recharge for sustainable groundwater development in Khapri watershed through recharge structures in succeeding chapter.